Supporting information for

A Ratiometric Fluorescent Molecular Probe with Enhanced Two-photon Response upon Zn^{2+} Binding for *in vitro* and *in vivo* Bioimaging

Kizhmuri P. Divya,[a,§] Sivaramapanicker Sreejith,[a,b,§] Pichandi Ashokkumar,[c] Kang Yuzhan,[d] Qiwen Peng,[d] Swarup Kumar Maji,[b] Yan Tong,[e] Hanry Yu,[d,f,g,] Yanli Zhao,[b,*] Perumal Ramamurthy[c] and Ayyappanpillai Ajayaghosh[a,*]*

[a] Photosciences and Photonics Group, Chemical Sciences and Technology Division, National Institute for Interdisciplinary Science and Technology (NIIST), CSIR, Trivandrum 695019 (India). Fax: (+91) 471-249-1712. E-mail: ajayaghosh@niist.res.in

[b] Division of Chemistry and Biological Chemistry
School of Physical and Mathematical Sciences, Nanyang Technological University, 21 Nanyang Link, 637371, Singapore. Email: zhaoyanli@ntu.edu.sg

[c] National Centre for Ultrafast Processes (NCUFP), University of Madras, Taramani Campus, Chennai 600113, India.

[d] Singapore-MIT Alliance for Research and Technology, 1 CREATE Way, #04-13/14, Enterprise Wing, #B-10, 138602, Singapore.

[e] Centre for Bioimaging Sciences (CBIS), Blk S1A, Level 2, Lee Wee Kheng Building, National University of Singapore, 14-Science Drive 4, 117557, Singapore.

[f] Department of Physiology, Yong Loo Lin School of Medicine, National University Health System, MD9, 2 Medical Drive, 117597 Singapore. Email: hanry_yu@nuhs.edu.sg

[g] Department of Biological Engineering, Massachusetts Institute Technology, Cambridge, MA02139, USA.

[§] These authors contributed equally to this work.

1. Experimental section

General

Solvents and reagents used were purified and dried by usual methods. All starting materials were obtained from commercial suppliers and used as received. All melting points were determined with a Mel-Temp-II melting point apparatus. ^{1}H and ^{13}C NMR spectra were measured on 300 and 500 MHz Bruker Avance DPX spectrometer or on a Varian Gemini 500 MHz spectrophotometer. Fluorescence quantum yield was determined using optically matching solutions of quinine sulphate ($\Phi_f = 0.54$ in 1N H_2SO_4) and rhodamine B ($\Phi_f = 0.7$ in ethanol) as standard and the quantum yield is calculated using equation 1.

$$\Phi_f = \Phi_r (A_r F_s / A_s F_r) (\eta_s^2 / \eta_r^2) \quad \ldots\ldots\ldots\ldots\ldots\ldots (1)$$

where, A_s and A_r are the absorbance of the sample and reference solutions, respectively at the same excitation wavelength, F_s and F_r are the corresponding relative integrated fluorescence intensities and η is the refractive index of the solvent.

Fluorescence lifetimes were measured using IBH (FluoroCube) time-correlated picosecond single photon counting (TCSPC) system. Solutions were excited with a pulsed diode laser (<100 ps pulse duration) at a wavelength of 375 nm (NanoLED-11) with a repetition rate of 1 MHz. The detection system consists of a microchannel plate photomultiplier (5000U-09B, Hamamatsu) with a 38.6 ps response time coupled to a monochromator (5000M) and TCSPC electronics (Data Station Hub including Hub-NL, NanoLED controller and preinstalled Fluorescence Measurement and Analysis Studio(FMAS) software). The fluorescence lifetime values were determined by deconvoluting the instrument response function with the decay using DAS6 decay analysis software. The quality of the fit has been judged by the fitting parameters such as χ^2 (< 1.2) as well as the visual inspection of the residuals.

The two-photon excitation was carried out using a mode locked femtosecond Ti: sapphire laser from Spectra Physics (Tsunami), with a repetition rate of 82 MHz and a pulse width of

about 100 femtoseconds. The tuning range of the Ti-Sapphire laser was 690 nm to 1080 nm. The output laser beam, with an average power of 0.6– 0.8 W, was vertically polarized. In the present study the standard optics with the output from 740 nm to 850 nm was used to excite the sample. The mode locked femtosecond laser was reflected onto a 10x objective, which focuses the laser beam into the sample and causes fluorescence. The multi-photon excited fluorescence was collected perpendicularly to the incident beam direction and measured using a single channel charge coupled detector spectrometer (Ocean Optics, model – USB4000-VIS-NIR) with the grating tuning range of 350 to 1000 nm. The two-photon excited emission was recorded using the Ocean Optics spectroscopy software (Spectrasuite).

The two photon action cross section is calculated using equation 2.

$$\delta\Phi_s = \delta\Phi_r C_r n_r F_s / C_s n_s F_r \quad \ldots\ldots\ldots\ldots\ldots\ldots \quad (2)$$

where, the subscripts 's' and 'r' refer to the sample and the reference solutions respectively. The terms '*C*' and '*n*' are the concentration and refractive index of the sample solution, respectively. '*F*' is the integrated two photon excited fluorescence intensity.

Two-photon images were taken using Leica TCS SP5X multi-photon microscope with the objective Leica HCX PL APO 40x/0.85 Corr and Chameleon Ultra II laser source.

2. Synthesis and Characterization

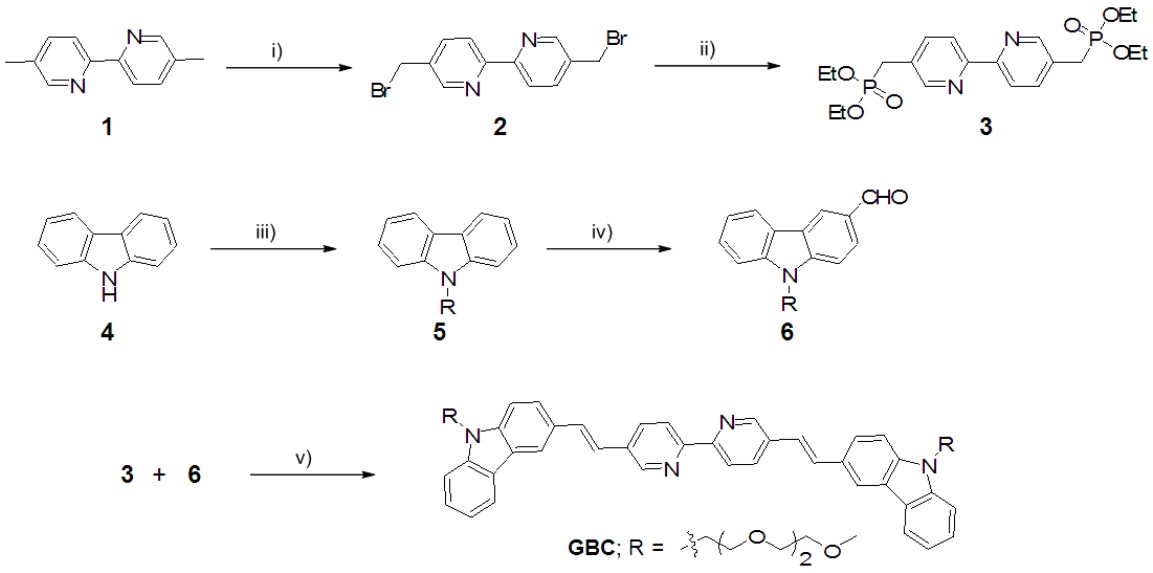

Scheme 1 Synthesis of **GBC**. Reagents and conditions; i) NBS, AIBN, CCl_4 18-20 h; ii) $P(OEt)_3$, 100 °C, 10-12 h; iii) 1-bromo-2-(2-(2-methoxyethoxy)ethoxy)ethane, NaH, THF-DMF, 32 °C, 21 h; iv) $POCl_3$, DMF, 0-32 °C, 12 h; v) NaH, THF, 32 °C, 12 h.

i) 5,5'-Bis(bromomethyl)-2,2'-bipyridine

To a solution of 5,5'-dimethyl-2,2'-bipyridine (**1**) (1.84 g, 10 mmol) in 50 mL of dry carbon tetrachloride was added *N*-bromosuccinimide (3.5 g, 20.5 mmol) and AIBN. The reaction mixture was refluxed for 18-20 h., cooled, filtered and the solvents were removed under reduced pressure to give the crude product which was further purified by recrystallization from CCl_4. Yield: 80-90%; m.p.: 188 °C; ^{1}H NMR ($CDCl_3$, 300 MHz, TMS): δ = 4.53 (s, 4H, -C*H*$_2$Br), 7.79 (m, 2H, Ar-*H*), 8.34 (m, 2H, Ar-*H*), 8.61 (m, 2H, Ar-*H*) ppm; ^{13}C NMR ($CDCl_3$, 75 MHz): δ = 29.43, 121.25, 133.28, 137.70, 149.27, 155.19 ppm.

ii) Preparation of 5,5'-Bis(diethyl phosphonomethyl)-2,2'-bipyridine

The bisphosphonate (**3**) was prepared by the reaction of the corresponding bisbromomethyl derivative (**2**) (680 mg, 2 mmol) with 3 mL of triethyl phosphite at 100 °C for 10-12 h followed by the removal of the unreacted triethyl phosphite under vacuum. Yield: 90-95%; ^{1}H NMR

($CDCl_3$, 300 MHz, TMS): δ = 1.12 (m, 12H, -C*H*$_3$), 3.21 (s, 4H, -C*H*$_2$P), 4.14 (m, 8H, -OC*H*$_2$-), 7.34 (m, 2H, Ar-*H*), 8.01 (m, 2H, Ar-*H*), 8.30 (m, 2H, Ar-*H*) ppm.

iii) 9-(2-(2-(2-Methoxyethoxy)ethoxy)ethyl)-9H-carbazole

A suspension of sodium hydride (290 mg, 12 mmol) in dry THF (50 mL) was added slowly to a solution of the 9H-carbazole, **4** (0.9 g, 2 mmol) in DMF. After stirring for 3 h, 1-bromo-2-(2-(2-methoxyethoxy)ethoxy)ethane (0.452 g, 2 mmol) was added to the reaction mixture. After stirring for 18 h, the crude product was obtained as a pasty residue by the removal of THF under reduced pressure. The residue was suspended in water and extracted with dichloromethane. The organic layer was washed with brine, dried over Na_2SO_4 and concentrated, which was further purified by column chromatography over silica gel using 10% ethyl acetate-petroleum ether as eluent. Yield: 60 %; ^{1}H NMR ($CDCl_3$, 300 MHz, TMS): δ = 8.36 (d, 2H, Ar-*H*), 7.70 (m, 4H, Ar-*H*), 7.37 (m, 2H, Ar-*H*), 4.50 (t, 2H, -NC*H*$_2$-), 3.85 (t, 2H, -NCH$_2$C*H*$_2$-), 3.54 (m, 8H, -OC*H*$_2$-), 3.30 (s, 3H, -OC*H*$_3$) ppm; ^{13}C NMR ($CDCl_3$, 75 MHz): δ = 134.1, 121.7, 109.6, 71.1, 70.4, 59.3, 57.4, 43.00 ppm; FAB: MS Calcd. for $C_{19}H_{23}NO_3$, 313.17; found 314.20.

iv) 9-(2-(2-(2-Methoxyethoxy)ethoxy)ethyl)-9H-carbazole-3-carbaldehyde

To a two-neck RB flask under argon atmosphere, $POCl_3$ (3.65 mmol) was taken and allowed to stir under ice-cold condition. Dimethyl formamide (DMF), (14.6 mmol) was added slowly into it. The reaction mixture was allowed to stir for 1 h. After the ylide formation (pale yellow color), 9-substituted carbazole (**5**) (3.18 mmol) was added slowly into the reaction mixture. After 12 h, the reaction mixture was poured into ice water in a beaker. A fresh solution of 0.5 N NaOH was added and heated up to 80 °C. The solution was then extracted with dichloromethane and purified using silica gel column chromatography (100-200 mesh, 30% ethylacetate-hexane as eluent). Yield: 45%; ^{1}H NMR ($CDCl_3$, 300 MHz, TMS): δ = 10.09 (s, 1H, -C*H*O), 8.61 (s, 1H, Ar-*H*), 8.17-8.14 (d, 1H, Ar-*H*), 8.02-7.99 (d, 1H, Ar-*H*), 7.55-7.44 (m, 3H, Ar-*H*), 7.34-7.29 (m, 1H, Ar-*H*), 4.51 (t, 2H, -NC*H*$_2$-), 3.88 (t, 2H, -NCH$_2$C*H*$_2$-), 3.54 (m, 8H, -OC*H*$_2$-), 3.32 (s, 3H, -

OCH_3) ppm; ^{13} C NMR ($CDCl_3$, 75 MHz): δ = 189.1, 139.8, 135.4, 126.7, 119, 109.6, 70.4, 59.4 ppm; FAB-MS: $[M]^+$ Calcd. for $C_{20}H_{23}NO_4$, 341.16; found 341.20.

v) 5,5'-Bis((E)-2-(9-(2-(2-(2-methoxyethoxy)ethoxy)ethyl)-9H-carbazol-3-yl)vinyl)-2,2'-bipyridine (GBC)

A suspension of sodium hydride (12 mmol) in dry THF (50 mL) was added slowly to a solution of the tetraethyl 2,2'-bipyridine-5,5'-diylbis(methylene)diphosphonate, **3** (2 mmol) and the *9*-substituted carbazole-2-carbaldehyde **6** (4 mmol) in THF. After stirring for 12 h, the fluorescent reaction mixture obtained was cooled followed by the removal of THF under reduced pressure to give a pasty residue. The residue was suspended in water and extracted with dichloromethane. The organic layer was washed with brine, dried over Na_2SO_4 and concentrated to give the crude product, which was further purified by column chromatography over basic alumina using 5% ethyl acetate-petroleum ether as eluent to get the solid product. Yield: 43-47%; m.p: 125-128 °C; ^{1}H NMR ($CDCl_3$, 500 MHz, TMS): δ = 8.81 (s, 2H, Ar-*H*), 8.43-8.42 (d, 2H, Ar-*H*), 8.26 (s, 2H, Ar-*H*), 8.14-8.12 (d, 2H, Ar-*H*), 8.04-8.02 (dd, 2H, Ar-*H*), 7.72-7.70 (dd, 2H, Ar-*H*), 7.49-7.46 (m, 8H, Ar-*H*), 7.29-7.26 (m, 2H, *J* = 15 Hz, vinylic-*H*), 7.19-7.16 (d, 2H, *J* = 15 Hz vinylic-*H*), 4.53-4.51 (t, 4H, -NCH_2-), 3.90-3.88 (t, 4H, -NCH_2CH_2-), 3.55-3.42 (m, 16H, -OCH_2CH_2-), 3.34 (s, 6H, -OCH_3) ppm; ^{13} C NMR ($CDCl_3$, 125 MHz): δ = 154.24, 147.94, 141.05, 140.80, 133.51, 132.98, 131.83, 128.19, 126.01, 124.61, 123.36, 122.92, 122.04, 120.88, 120.40, 119.44, 118.95, 109.36, 109.17, 71.85, 71.01, 70.01, 70.62, 70.55, 69.34, 59.00, 43.34 ppm; FAB-MS: $[M]^+$ Calcd. for $C_{52}H_{54}N_4O_6$, 830.40; found 832.66.

3) Photophysical Studies

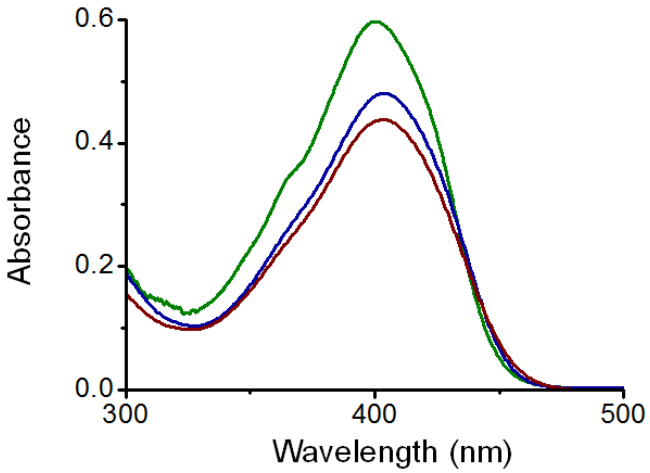

Fig. S1 Absorption spectra of **GBC** (6×10^{-6} M) in $CHCl_3$ (——), acetonitrile (——), 1:1 acetonitrile/water (HEPES, pH 7.2) (——).

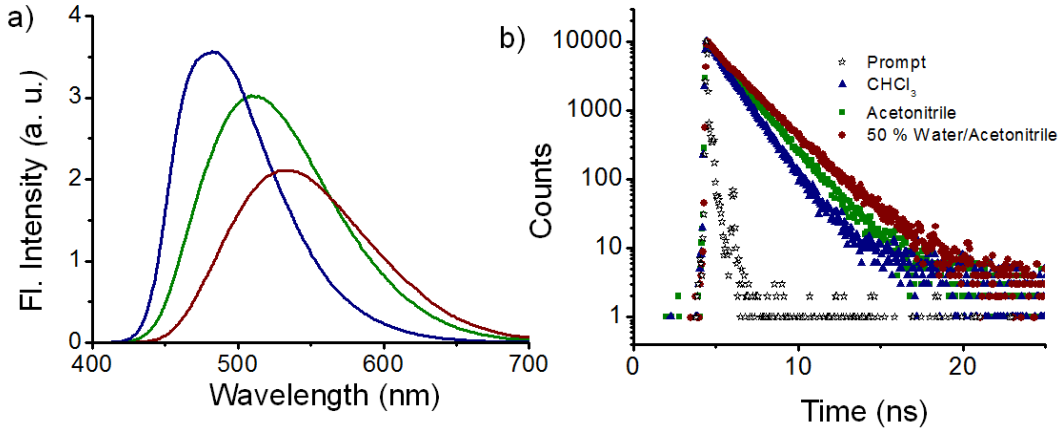

Fig. S2 Emission spectra of **GBC** (6×10^{-6} M; λ_{ex}= 400 nm) in $CHCl_3$ (——), acetonitrile (——), 1:1 acetonitrile/water (HEPES, pH 7.2) (——). b) Fluorescence lifetime decay profiles of GBC in various solvents (Fluorescence decay profiles were recorded by excitation at 375 nm, emission monitored at the emission maximum).

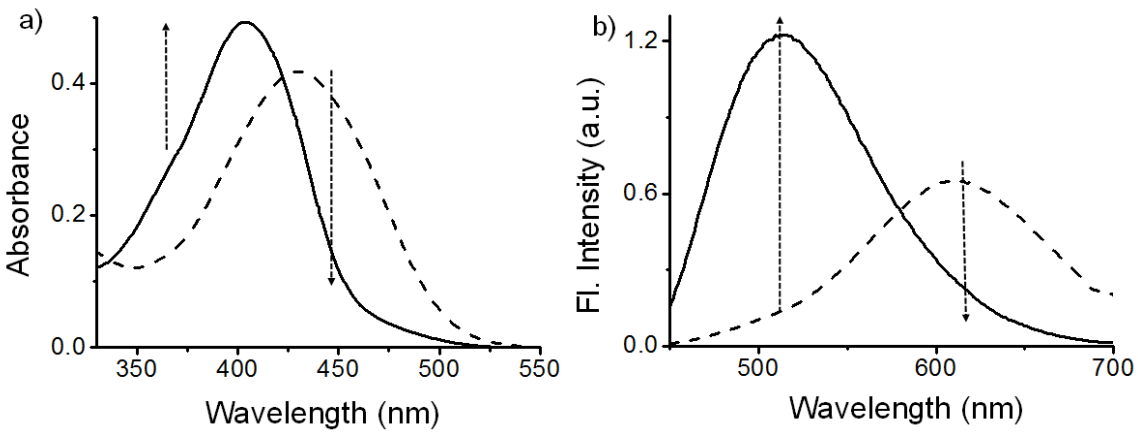

Fig. S3 Changes in the a) absorption and b) emission spectra of **GBC•Zn**$^{2+}$ (---) (Conc. 6 μM) with the addition of EDTA (—) (2×10^{-5} M) in 1:1 acetonitrile /water (HEPES, pH 7.2) ex @ 422 nm.

4) Metal Ion Binding and Selectivity Studies

Addition of Cd^{2+} to a 1:1 acetonitrile/water (HEPES, pH 7.2) solution of **GBC** resulted in a new emission peak at 590 nm (Figure S5) indicating that GBC is sensitive to both Zn^{2+} and Cd^{2+}. However, interference with Cd^{2+} may not be a serious problem with the analysis of biological samples since Cd^{2+} is not a biological cation.

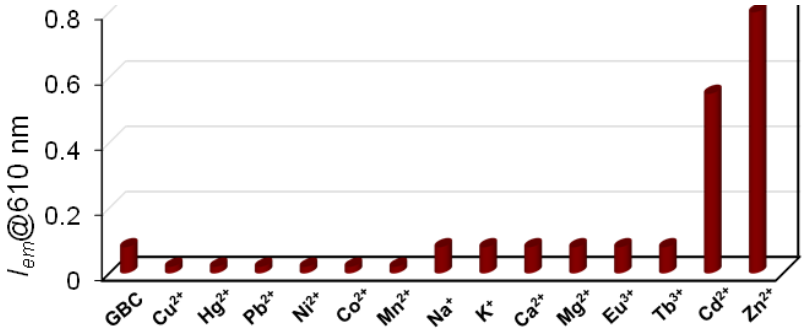

Fig. S4 Plot of fluorescence intensity of GBC monitored at 610 nm with different metal ions in acetonitrile/water (HEPES, pH 7.2), 1:1 mixture.

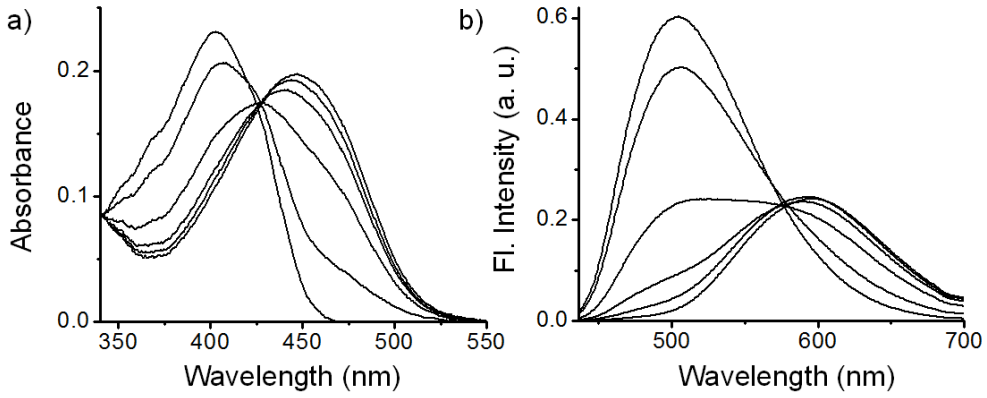

Fig. S5 Changes in the a) absorption and b) emission spectra of **GBC** (6 μM) with the addition of $Cd(ClO_4)_2$ (0-6 μM) in 1:1 acetonitrile /water (HEPES, pH 7.2) ex @ 422 nm.

5) Photostability Test

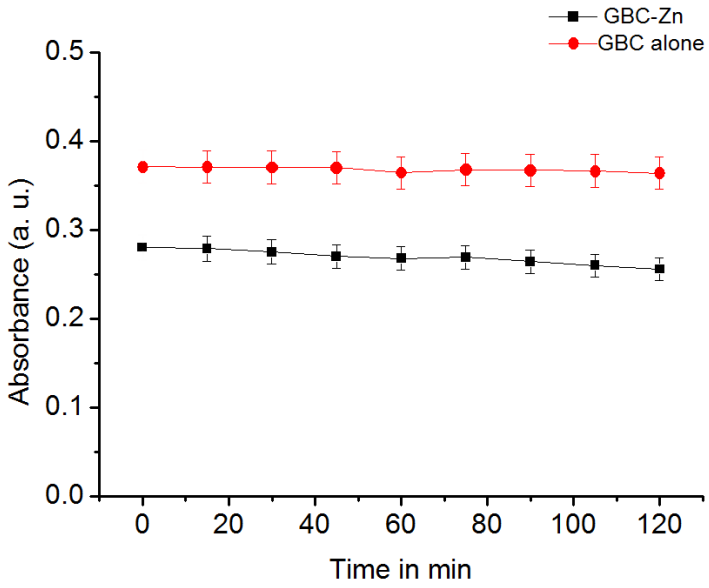

Fig. S6 Plot of absorption changes of GBC (6×10^{-6} M) in acetonitrile/water (HEPES, pH 7.2), 1:1 mixture by irradiating with 808 nm continuous laser source in a quartz cuvette.

6) *In vitro* Cytotoxicity Assay

HeLa cells were seeded into a 96-well plate (1×10^4 cells per well) in DMEM (Dulbecco's Modified Eagle's Medium) cell culture medium containing 10% fetal bovine serum (FBS), 100 U mL^{-1} penicillin and 100 $mgmL^{-1}$ streptomycin, and grown under a humidified atmosphere with 5% CO_2 at 37°C. After 12 h incubation, the media in the wells were replaced with fresh DMEM media (100 μL per well) containing GBC with different concentrations, and the cells were further incubated for 12 h. Then, the medium was changed by DMEM (100 μL per well) containing MTT (0.5 $mgmL^{-1}$), followed by incubation for another 4 h. The culture medium was removed and frozen crystals were dissolved with freshly prepared DMSO (100 μL). Before the cytotoxicity measurement, the plate was agitated gently for 15 min, and then the absorbance intensity at 560 nm was recorded by a micro plate reader (Infinite 200 PRO, Tecan). The relative cell viability (%) for each sample related to the control well was finally calculated.

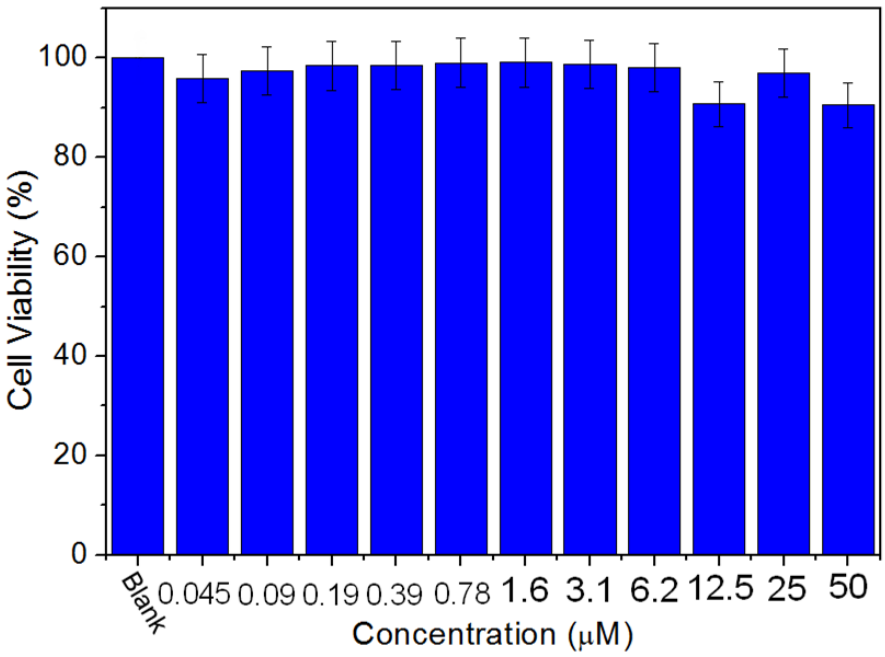

Fig. S7 Cytotoxicity studies of GBC using 3-(4,5-dimethlthiazol-2-yl)-2,5-diphenyltetrazolium bromide (MTT) assays in HeLa (human cervix adenocarcinoma) cell lines.

7) *In vivo* 2P imaging

This study is conform with the Guide for the Care and Use of Laboratory Animals published by the National Institutes of Health, USA, and the protocol is approved by the Institutional Animal Care and Use Committee (IACUC), National University of Singapore.

Step 1: Anaesthetized a rat with Ketamine/Xylazine intraperitoneally in an animal chamber. After the animal had lost its foot pad reflex, an incision along the vertical middle line was made to expose the left lobe. The incision of the upper abdomen was sutured (3-0 prolene suture), leaving a part open to create a circled wound to position the liver window device (diameter 1.2cm) inside the abdominal wall. Prior to installing the lid, a cover glass was adhered around the outer rim by using biocompatible glue. The cover glass serves as the observation window of intra-vital activities. The lid was then interrupted and sutured through the small holes on the ring to the skin and peritoneum. To ensure tight contact of the liver surface with the cover glass and to minimize motional artifacts associated with heartbeat and respiration, tissue adhesive was applied to the edge of the lid to adhere the liver to the imaging chamber. *Step 2*: Opened the skin of neck and exposed the right jugular vein to make a small incision and inserted a catheter. Secured the catheter with 5/0 suture, and closed the skin using 3/0 prolene. *Step 3*: Fixed the animal on the microscopy stage and injected the corresponding probes through the catheter.

8) Survey and Comparison with Previous Literature Reports

Table S1 Comparison of 2PA and 2PEF properties of known ligands and their Zn^{2+} complexes.

	Ligand		Ligand+Zn^{2+}		Remarks
	δ (GM)	δΦ (GM)	δ (GM)	δΦ (GM)	
2[a]	31 (690 nm)	11	77 (730 nm)	55	Ratiometric
TPPA[b]	ND	ND	ND	193	Ratiometric 11.5 fold compared to TPPA alone
DZn[c,]	400 (810 nm)	8	935	580	Non ratiometric
AD1[d]	ND	ND	5 (720 nm)	ND	Non ratiometric
AD2[d]	133 (800 nm)	ND	205 (840 nm)	ND	Ratiometric
6-MPVQ[e]	335 (710 nm)	ND	470	ND	Ratiometric
6-MPQ[e]	135 (725 nm)	ND	250	ND	Ratiometric
AZn1[f]	ND	ND	210 (780 nm)	86	Non ratiometric
AZn2[f]	ND	ND	140 (780 nm)	95	Non ratiometric
FluZin[f]	ND	ND	55	24	Non ratiometric
TSQ[f]	ND	ND	10	4	Non ratiometric
SZn-Mito[g]	ND	ND	82	75	7-fold compared to SZn-Mito alone
SZn2-Mito[h]	ND	ND	ND	155	Non ratiometric
GBC[i]	**107 (800 nm)**	**95**	**1433 (815 nm)**	**860**	**Ratiometric**

ND: not determined

(*a*) S. Sumalekshmy, M. M. Henary, N. Siegel, P. V. Lawson, Y. Wu, K. Schmidt, J.-L. Brédas, J. W. Perryl and C. J. Fahrni, *J. Am. Chem. Soc*., 2007, **129**, 11888-11889; (*b*) A. Bhaskar, G. Ramakrishna, R. J. Twieg and T. J. Goodson III, *J. Phys. Chem. C* 2007, **111**, 14607-14611; (*c*) C. Huang, J. Qu, J. Qi, M. Yan and G. Xu, *Org. Lett*., 2011, **13**, 1462-1465; (*d*) L. Xue, Z. Fang, G. Li, H. Wang and H. Jiang, *Sens. Actuators B* 2011, **156**, 410–415; (*e*) X. Meng, S. Wang, Y.

Li, M. Zhu and Q. Guob, *Chem. Commun*., 2012, **48**, 4196–4198; (*f*) H. M. Kim, M. S. Seo, M. J. An, J. H. Hong, Y. S. Tian, J. H. Choi, O. Kwon, K. J. Lee and B. R. Cho, *Angew. Chem., Int. Ed*. 2008, **47**, 5167-5170; (*g*) G. Masanta, C. S. Lim, H. J. Kim, J. H. Han, H. M. Kim and B. R. Cho, *J. Am. Chem. Soc*., 2011, **133**, 5698–5700; (*h*) N. Y. Baek, C. H. Heo, C. S. Lim, G. Masanta, B. R. Cho and H. M. Kim, *Chem. Commun*., 2012, **48**, 4546-4548; (*i*) **Present work**.